J. For. Res. (2021) 32:1599–1611
https://doi.org/10.1007/s11676-020-01195-7

ORIGINAL PAPER

Morphological and kinetic parameters of the absorption of nitrogen forms for selection of *Eucalyptus* clones

Matheus Severo de Souza Kulmann[1] · Betania Vahl de Paula[1] · Paula Beatriz Sete[2] · Wagner Squizani Arruda[1] · Gabriel Alberto Sans[1] · Camila Peligrinotti Tarouco[3] · Luciane Almari Tabaldi[3] · Fernando Teixeira Nicoloso[3] · Gustavo Brunetto[1]

Received: 18 October 2019 / Accepted: 23 May 2020 / Published online: 30 July 2020

Abstract *Eucalyptus* clones are selected according to productivity, wood quality, rooting capacity, and resistance to drought, frost and diseases. However, kinetic and morphological parameters that determine the absorption efficiency of nutrients such as nitrate (NO_3^-) and ammonium (NH_4^+) are often not considered in breeding programs. The objective of this study was to evaluate the morphological, physiological and kinetic parameters of nitrogen uptake by clones of *Eucalyptus saligna* (32,864) and *Eucalyptus grandis* (GPC 23). Morphological parameters in shoot and root systems, biomass and N concentrations in different organs, photosynthetic pigment concentrations, parameters of chlorophyll *a* fluorescence and photosynthetic rates were evaluated. Kinetic parameters, maximum absorption velocity (V_{max}), Michaelis–Menten constant (K_m), minimum concentration (C_{min}) and influx (I) were calculated for NO_3^- and NH_4^+ in the two clones. *E. grandis* clone was more efficient in the uptake of NO_3^- and NH_4^+, and showed lower K_m and C_{min} values, allowing for the absorption of nitrogen at low concentrations due to the high affinity of the absorption sites of clone roots to NO_3^- and NH_4^+. Higher root lengths, area and volume helped the *E. grandis* clone in absorption efficiency and consequently, resulted in higher root and shoot biomass. The *E. saligna* clone had higher K_m and C_{min} for NO_3^- and NH_4^+, indicating adaptation to environments with higher N availability. The results of NO_3^- and NH_4^+ kinetic parameters indicate that they can be used in *Eucalyptus* clone selection and breeding programs as they can predict the ability of clones to absorb NO_3^- and NH_4^+ at different concentrations.

Keywords Ammonium and nitrate · *Eucalyptus saligna* · *Eucalyptus grandis* · Root system architecture · Nitrogen influx · Maximum absorption velocity (V_{max}), Michaelis–Menten constant (K_m) and Minimum concentration (C_{min})

Introduction

The global area of plantations continues to increase rapidly to address consumption demands for forest products. However, plantations provided only 39% of the world's wood requirements in 2015 (FAO 2016), therefore highlighting the opportunity for plantations to satisfy current and future wood demands (Paquette and Messier 2010). Forest plantations occupy approximately 290.4 million ha worldwide (FAO 2016), of which 20 million ha are *Eucalyptus* (Booth 2013). Among the eucalypt species used for reforestation, *Eucalyptus grandis* W. Hill and *Eucalyptus saligna* Sm. are economically important because they are tolerant to cold temperatures and mild frosts, as well as being fast growing and having high quality wood (Gonçalves et al. 2013).

Eucalyptus clone plantations are commonly established on sandy-textured soils (Iglesias and Wilstermann 2008)

Project funding: The work was funded partly by the Conselho Nacional de Desenvolvimento Científico and Tecnológico (CNPq).

The online version is available at https://www.springerlink.com.

Corresponding editor: Tao Xu.

✉ Gustavo Brunetto
brunetto.gustavo@gmail.com

[1] Soil Science Department, Federal University of Santa Maria, Santa Maria, RS 97105-900, Brazil

[2] Federal University of Santa Catarina, Admar Gonzaga Highway, 1346, Florianópolis, SC 88034-001, Brazil

[3] Biology Department, Natural and Exact Sciences Center, Federal University of Santa Maria, Santa Maria, RS 97105-900, Brazil

with low organic matter and low levels of natural nitrogen (N). However, *Eucalyptus* clones used in commercial plantations are selected for their productivity, desirable wood qualities, rooting ability, and resistance to drought, cold, frost and diseases (Gonçalves et al. 2013). However, kinetic parameters related to nutrient uptake efficiency such as nitrogen in the form of nitrate (NO_3^-) and ammonium (NH_4^+) are not generally considered, although N is a major nutrient that affects the growth and development of *Eucalyptus*. Nitrogen is a primary constituent of important plant components such as proteins, nucleic acids, adenosine 5-triphosphate (ATP), nicotinamide adenine dinucleotide (NADH), nicotinamide adenine dinucleotide phosphate (NADPH), chlorophyll, enzymatic cofactors, phytohormones, and secondary metabolites (Marschner 2012; Tomasi et al. 2015). Based on the importance of nitrogen, *Eucalyptus* clones with higher N uptake efficiencies will be important contributors to breeding programs and will impact positively on higher wood yields.

N uptake by plants is generally in the mineral forms NO_3^- and NH_4^+, mediated by transport proteins or transporters in the plasma membranes of the epidermis and root cortex cells (Marschner 2012). The functioning of the transporters varies according to the affinity for NO_3^- and NH_4^+, and can be classified as high affinity (HATS), low affinity (LATS) or double affinity. In general, HATS proteins are activated at low concentrations as ions in solution (< 0.5 mmol L^{-1}), while LATS act at higher concentrations (> 0.5 mmol L^{-1}). The molecular basis of these absorption systems has been described for *Arabidopsis* (Dechorgnat et al. 2010) and identified in forest species (Kronzucker et al. 1995) and fruit species (Pii et al. 2014; Tomasi et al. 2015). Based on this, NO_3^--LATS and NO_3^--HATS were encoded in two gene families, NRT1 and NRT2, respectively, except for NRT1.1, a dual affinity transporter (Pii et al. 2014; Tomasi et al. 2015), and for NH_4^+-LATSs and NH_4^+-HATS, belonging to the subfamily AMT2 and AMT1, respectively (Couturier et al. 2007). Therefore, it is expected that plants will adapt to conditions of low nutrient availability in order to trigger high affinity systems, especially with nitrogen (Castro-Rodríguez et al. 2017; Xuan et al. 2017).

Kinetic parameters of nutrient absorption are the maximum absorption rate (V_{max}), the minimum concentration (C_{min}), the Michaelis–Menten constant (K_m), and the influx (I) (Yang et al. 2007; Martinez et al. 2015). $V_{\max}$ is the saturation point of root cell membrane transport sites by absorbed ions; C_{min} is the minimum nutrient concentration in the solution for roots to initiate absorption; and, K_m is a parameter that describes the affinity of the ions to the transporter system. A smaller K_{m} demonstrates greater ion affinity with the transport sites. I is the inflow or velocity of ion absorption in a concentration solution (Martinez et al. 2015; Alves et al. 2016).

Nitrogen absorption by plants is important for many physiological processes, especially in the biosynthesis of essential proteins and enzymes involved in photosynthesis such as the enzyme Rubisco which results in higher CO_2 assimilation and contributes to the efficient use of water and nutrients (Tcherkez et al. 2017; Nadal and Flexas 2018). Under high light conditions, the enzyme responsible for reducing NO_3^- in the assimilation process is activated, stimulating absorption (Marschner 2012). This occurs by the acquisition of light signals through the leaf and their transmission to other organs to contribute to the development of the root system and increases the absorption of water and nutrients such as nitrogen (Lee et al. 2016). Light signals received by the shoots also regulate root development through the transfer of signaling molecules from shoots to roots. Activation of phytochrome A (phyA) and phytochrome B (phyB) acts as photoreceptors and transduces light signals from shoots to roots, resulting in auxin biosynthesis or redistribution in the root system, thereby stimulating root development, especially the production of lateral roots (Lee et al. 2016). PhyB induces the expression of *ELONGATED HYPOCOTYL* 5 (HY5) and promotes stabilization of the HY5 protein which moves from the shoots to the roots where it activates gene- encoding NO_3^- transporters, increasing its uptake (Lee et al. 2016; Xuan et al. 2017).

Kinetic parameters may assist in the identification of plants that are well-adapted to different edaphoclimatic conditions. Rates of N absorption have been reported for annual crops such as rice (Araújo et al. 2015), corn (Horn et al. 2006), barley (Glass 2003) and Chinese cabbage (Song et al. 2016), and for fruit species such as grapevine (Tomasi et al. 2015) and peach (de Paula et al. 2018). However, for tree species, in particular *Eucalyptus* clones, little is known about NO_3^- and NH_4^+ absorption kinetic parameters. Therefore, it is expected that *Eucalyptus* clones possess different abilities to absorb NO_3^- and NH_4^+, and this will be reflected in the absorption efficiency and nutrient use and, consequently, in the physiological responses during growth and production. The selection of the most efficient *Eucalyptus* clones for NO_3^- and NH_4^+ uptake is recommended for low nitrogen soils, while the least efficient NO_3^- and NH_4^+ uptake clone but with important wood characteristics for the consumer market is recommended for soils with higher N levels (Clough et al. 2013; Rocha et al. 2014). As a result, the ideal *Eucalyptus* clone for plantations in low N soils has low C_{min} and K_m values and high V_{max} values, and consequently higher I (Martinez et al. 2015). The results from this study may contribute to the selection of *Eucalyptus* clones with greater nutrient absorption capacities and zoning of clones best adapted to the soil conditions of each region, thereby contributing to increasing productivity. The objective is to select *Eucalyptus* clones according to their

efficiency of N absorption using kinetic, physiological and morphological parameters.

Material and methods

Plant material and treatments

The experiment was conducted from September to October 2017 in the greenhouse at the Department of Soils of the Federal University of Santa Maria (UFSM), Santa Maria, Rio Grande do Sul, southern Brazil. Throughout the experiment, average temperatures of 25 °C and average relative humidity of 60% were maintained. Seedlings of *E. saligna* (32,864) and *E. grandis* (GPC 23) clones were produced from shoots from cut matrices. Mini-cuttings of shoot branches were collected and rooted in the greenhouse. The mini-cuttings were 12-cm long with three superior buds; leaves were cut to the center of the leaf midrib, leaving 50% of the photosynthetic area and reducing the amount of transpiration. Cultivation containers were nontoxic polypropylene plastic tubes with a volume of 180 cm^3, containing substrate (1:1:1 v:v:v) of carbonized rice husks, vermiculite and a commercial substrate of pine bark. In August 2017, 60-d clones approximately 20-cm high were transferred to polyethylene bags and stored in a greenhouse at 10 cm × 15 cm spacing. At 90 days, five *E. saligna* (32,864) and *E. grandis* (GPC 23) plants approximately 40-cm in height and with 10 to 15 leaves were removed from the plastic bags, their roots washed and transferred to 8-L pots with 5 L of 25% full strength Hoagland nutrient solution (Jones 1983) where they remained for seven days until the first acclimatization step was accomplished. The 100% Hoagland nutrient solution contained (in mg L^{-1}) NO_3^- = 196; NH_4^+ = 14; P = 31; K = 234; Ca = 160; Mg = 48.6; S = 70; Fe-EDTA = 5; Cu = 0.02; Zn = 0.15; Mn = 0.5; B = 0.5; and Mo = 0.01.

The pots were placed in the greenhouse in a completely randomized design with five replications per treatment, each plant considered a repetition. A Styrofoam slice was fixed on the surface of each pot to fasten the plants, preventing the entry of solar radiation and reducing the evaporation of the solution. The Styrofoam blade had a central hole for the *Eucalyptus* clone stem pass through and a second hole for the entrance of a PVC (polyvinyl chloride) tube connected to an oil-free air compressor for aeration.

After 7-d acclimatization of the clones in Hoagland solution, the solution was exchanged and the plants remained for 21 d in 50% full strength Hoagland nutrient solution, finishing the second acclimatization period. The solution was renewed every five days with the pH adjusted to 6.0 ± 0.2 through the addition of 1 mol L^{-1} HCl or 1 mol L^{-1} NaOH every two days. After the periods of acclimatization, the clones were induced to exhaustion nutrient reserves in a 0.1 mol L^{-1} $CaSO_4$ solution for 30 d. Where Ca and S were used to maintain the electrochemical potential of cell membranes and preserve cell wall integrity (de Paula et al. 2018).

Net absorption kinetics of NO_3^- and NH_4^+

After 30-d the exhaustion of nutrient reserves in a $CaSO_4$ solution (0.1 mol L^{-1}), the clones were returned to the Hoagland solution at 50% full strength and kept in this solution for 1 h for the system to reach steady absorption state conditions for the application of the kinetic model by Claassen and Barber (1974). Following this, the solution was replaced again, containing the same concentration of nutrients of 50% Hoagland solution to collect the first aliquots of the solution itself. Every six hours a 10-mL solution was collected from each 5 L pot at time zero before adjusting the plants in the pots with an initial solution. Aliquots of 10 mL were collected every six hours beginning at the first 30 h, every three hours between 30 and 54 h, and every hour between 54 and 65 h. The solutions were frozen at − 10 °C and stored for further analysis of N compounds.

Photosynthetic parameters

The evaluation of these parameters was carried out on the third fully expanded leaf using an infra-red gas analyzer (IRGA) portable meter (Li-Cor, LI-6400 XT, United States) and 1,500 µmol m^{-2} s^{-1} photosynthetic active radiation and a CO_2 concentration of 400 µmol mol^{-1}. Measurements were taken between 8:00 and 10:00 am to obtain net photosynthetic rate (A-µmol CO_2 m^{-2} s^{-1}), stomatal conductance of water vapor (Gs-µmol H_2O m^{-2} s^{-1}), intercellular concentration of CO_2 (Ci-µmol CO_2 mol^{-1}), the transpiratory rate (E-mmol H_2O m^{-2} s^{-1}) and instantaneous water use efficiency (WUE-µmol CO_2 mol^{-1} H_2O). These were recorded as the ratio between the CO_2 fixed by photosynthesis and the amount of transpired water and the efficiency of rubisco carboxylation (A/Ci-mol CO_2 m^{-2} s^{-1}). The ratio between the CO_2 fixed by photosynthesis and the internal concentration of CO_2.

Evaluation of chlorophyll *a* fluorescence

Chlorophyll *a* fluorescence was analyzed on the first fully expanded leaf of three plants per treatment on sunny mornings between 8:00 and 9:30 am (Souza et al. 2013) using a portable fluorometer of modulated light (Junior-Pam Chlorophyll Fluorometer Walz Mess-und-Regeltechnik, Germany). Prior to measurements, the leaves were pre-adapted to darkness for 30 min to measure initial fluorescence (F_o). Subsequently the samples were subjected to a saturating light pulse (10,000 µmol m^{-2} s^{-1}) for 0.6 s. The maximum quantum yield of PSII (F_v/F_m) was obtained as the ratio between

variable fluorescence ($F_v = F_m – F_o$) and maximum fluorescence. The photochemical quenching coefficient (qP) was calculated as $(F_m' – F_s)/(F_m' – F_o')$ (Schreiber et al. 1995). The electron transport rate (ETR_m) was evaluated using induction curve fluorescence (1,500 mmol m^{-2} s^{-1}).

Photosynthetic pigment determination

Leaves used to evaluate chlorophyll *a* fluorescence were collected and frozen in liquid N_2 for photosynthetic pigment analysis. Chlorophyll *a* (Chl *a*), chlorophyll *b* (Chl *b*) and carotenoid contents were analyzed according Hiscox and Israeslstam (1979), and estimated with Lichtenthaler's formula (Lichtenthaler 1987). Fresh 0.05 gm leaf samples were incubated in 7.0 mL of dimethyl sulfoxide (DMSO) at 65 °C for two hours until the tissues were completely bleached. Pigment concentrations were calculated after absorbance reading on a Celm E-205D spectrophotometer (Bel Engineering, Italy) at 645 and 663 nm for Chl *a* and Chl *b*, respectively, and 470 nm for carotenoids. Chlorophyll and carotenoid concentrations were expressed as mg g^{-1} fresh weight.

Plant collection and analysis of N concentration in tissues and solution

After 65-h kinetic gait evaluation, the plants were removed from the nutrient solution and fractionated into leaves, stem and roots. Height was measured and stem diameter determined using a manual caliper. Fresh root and shoot matter were weighed and the volume of nutrient solution remaining in each pot was measured. The materials were dried in an air-forced ventilation oven at 65 °C until constant mass, and then weighed to determine dry matter.

The plant tissues were ground in a 2-mm Willey mill, weighed and nitrogen concentrations determined using an elemental analyzer (FlashEA 1112, Thermo Electron Corporation, Italy). NO_3^- and NH_4^+ of the 65-h solutions were determined colorimetrically using a Segmented Flow Analyzer System (SAN^{++} System, Skalar, Netherlands).

Root system morphology

The characterization of root morphology was obtained from digitized images using an EPSON Expression 11,000 scanner equipped with additional light (TPU) with a 600 dpi resolution. The scanned images were used to determine root morphological traits using the WinRHIZO Pro software (Regent Instrument Inc., Canada). Total root length (cm ind.$^{-1}$), surface area (cm^2 ind.$^{-1}$), volume (cm^3 ind.$^{-1}$), average diameter (mm) and percent distribution of fine root length (*L*) for each diameter class (%) of $0 < L \leq 0.2$; $0.2 < L \leq 0.45$; $0.45 < L \leq 0.75$; $0.75 < L \leq 1.5$; $L > 1.5$, were obtained.

Statistical analysis

Kinetic parameter (V_{max} and K_m) values were calculated according to the NO_3^- and NH_4^+ concentrations in the Hoagland solution, the initial and final solution volumes in the pots, and root fresh matter values using the software Influx. C_{min} was determined according to the concentrations of NO_3^- and NH_4^+ in the nutrient solution corresponding to the 65 h of evaluation time. Influx (*I*) was calculated using Eq. 1 by Michaelis–Menten and modified by Nielsen and Barber (1978).

$$I = \left[\frac{V_{max} \times (C - C_{min})}{K_m + (C - C_{min})} \right] \quad (1)$$

where, V_{max} is membrane transporters' maximum absorption rate; *C* is the concentration in solution at collection time; C_{min} is the minimum concentration at the 65-h period and K_m is transporter affinity coefficient per solute.

The results from the morphological and physiological parameters were submitted to homogeneity and normality tests and subsequently, the data were processed and statistically analyzed using R statistical software (R Development Core Team 2019). When the effects of the treatments were considered significant, the results of V_{max}, K_m, C_{min} and *I* for each *Eucalyptus* clone were compared by Student's *t*-test ($P < 0.05$). The difference in NH_4^+ and NO_3^- concentrations over 65 h for each clone was compared by the Scott Knott test ($P < 0.05$), as this test is better suited to 25 times of solution collection.

Additionally, the data were also subjected to principal component analysis (PCA) using Canoco software version 4.5 (Ter Braak and Smilauer 2002). PCA is generally used to find the weight of each variable to maximize the variance among sampling points (Ortega et al. 1999). Principal componsent analysis is performed according to a set of principal components (PC1 and PC2) which are composed of standardized orthogonal linear combinations that together explain the variance of the original data. This type of analysis allows for the identification of more complex interactions between the evaluated variables and those with greater contribution to the differences among treatments.

Results and discussion

Morphological parameters

The *E. grandis* clone had higher values for height, dry matter production of leaves, roots, and total dry matter and

the highest levels of N in leaves and roots compared with the *E. saligna* clone (Table 1), suggesting that the higher dry matter production of the *E. grandis* shoots may have increased transpiration, generating a higher water gradient between the solution and the plant, stimulating N uptake by roots (Zufferey et al. 2015; Lee et al. 2016). Lower values of accumulated N and dry matter in leaves and roots of *E. saligna* may be attributed to lower efficiency of the clone in absorbing N which reduces nitrogen translocation to growing organs, resulting in lower heights and biomass production. Lower biomass production results from a reduction in light interception capacity, fixing less carbon which reduces the concentration of photoassimilates and absorbing less nutrients from the roots (Marschner 2012; Lee et al. 2016; Canarini et al. 2019).

The *E. grandis* clone had greater length, surface area, root volume and percentage distribution of fine roots (< 1.5 mm in diameter) than *E. saligna* (Fig. 1a, b, d, e), variables that determine the absorption rate of water and nutrients by the roots (Batista et al. 2016). The higher fine root production of the clone may have been the result of the greater reception of light signals by the shoots and transfer via signaling molecules to the roots (Lee et al. 2016), since the clone showed greater shoot growth (Table 1). Reception of these light signals activates the production of fine roots, increasing contact with water (Skaggs and Shouse 2008) and nutrients (Lambers et al. 2006). The greater fine root production by the clone may be a strategy to increase the area of soil/solution with lower carbon investment. In addition, the accumulation of N in the roots promotes the growth of *Eucalyptus* clones, since roots are sinks of carbohydrates and amino acids used to overcome nutrient deficiency conditions and thus be redistributed to growing organs (Centinari et al. 2016; Klodd et al. 2016).

Table 1 Morphological parameters, accumulation and total N content in tissues of *E. grandis* and *E. saligna* clones after 30-d reduced internal nutrient reserves

Parameters	*E. grandis*	*E. saligna*
Height (cm)	51.3 ± 1.3 * [(a)]	47.3 ± 2.1
Stem diameter (cm)	0.3 ± 0.1 ns	0.4 ± 0.1
Leaves dry matter (g)	0.5 ± 0.1 **	0.2 ± 0.0
Stem dry matter (g)	1.1 ± 0.2 [ns]	0.7 ± 0.2
Root dry matter (g)	0.7 ± 0.1 *	0.3 ± 0.1
Total dry matter (g)	2.3 ± 0.3 *	1.1 ± 0.2
Root/shoot ratio (g)	0.5 ± 0.1 ns	0.3 ± 0.2
Total N in leaves (%)	2.9 ± 0.5 ns	3.4 ± 0.3
Total N in stems (%)	0.9 ± 0.1 ns	0.8 ± 0.1
Total N in roots (%)	1.4 ± 0.1 ns	1.4 ± 0.2
N accumulated in leaves (g organ^{-1})	1.5 ± 0.4 *	0.5 ± 0.1
N accumulated in stems (g organ^{-1})	0.9 ± 0.2 [ns]	0.6 ± 0.2
N accumulated in roots (g organ^{-1})	1.0 ± 0.3 *	0.4 ± 0.1

[(a)] Means ± SD followed by statistical significance [* = Significant by Student's *t*-test ($P < 0.05$); ** = Significant by Student's *t*-test ($P < 0.01$); ns = not significant ($P < 0.05$)]

Kinetic parameters of NO_3^- and NH_4^+ absorption

The *E. grandis* clone had lower K_m and C_{min} values for NO_3^- compared to the *E. saligna* clone (Fig. 2a). The C_{min} results suggest that *E. grandis* has NO_3^- transporter proteins that are activated at lower ion concentrations in solution, and the low K_m values show high affinity for NO_3^-. In addition, the *E. grandis* clone had the largest length, surface area and root volume compared to the *E. saligna* clone (Fig. 1a, b, d), which contributed to the higher number of transporter proteins of NO_3^- and N absorption efficiency (Lambers et al. 2006; Raven et al. 2018; Canarini et al. 2019). The smaller C_{min} values suggest that the *E. grandis* clone has a higher absorption ability even in small concentrations of NO_3^- in the environment (solution or soil), and can access NO_3^- on a larger number of absorption sites per root unit in different environments relative to the *E. saligna* clone (Tomasi et al. 2015; Batista et al. 2016). This suggests that the *E. grandis* clone may be grown in solution or in soils with lower NO_3^- availability, which may occur in soils with less history of fertilizer application or in soils with low organic matter (Clough et al. 2013). As a result, the risk of contamination of surface and subsurface waters by NO_3^- adjacent to areas cultivated with *Eucalyptus* is also reduced (Bindraban et al. 2015; Bednorz et al. 2016). On the other hand, *E. grandis* and *E. saligna* clones did not differ statistically between V_{max} values for NO_3^-, indicating that these clones have similar nutrient absorption properties in solution when all loader sites in the root cell membranes are saturated (Yang et al. 2007; Martinez et al. 2015).

NO_3^- absorption kinetics shows the differentiation in absorption between the clones as illustrated by the clone influx curve (Fig. 2a). *E. grandis* clone initiates absorption of NO_3^- in solution even at low concentrations and continues absorption even at higher levels compared to *E. saligna*, and therefore has lower C_{min} values (Fig. 2a). This shows that different *Eucalyptus* clones absorb NO_3^- through distinct transport systems. Thus, the *E. grandis* clone possibly activates a high affinity system (HATS), while the *E. saligna* clone may activate a low affinity system (LATS), each mediated by more than one membrane protein with different enzymatic kinetics. The molecular basis of these high and low affinity absorption systems has been identified (Dechorgnat et al. 2010), mainly in the *Arabidopsis* model plant (Doddema and Telkamp 1979), demonstrating that a LATS belongs to the NRT1 transporter family and a HATS to the NRT2 family, except for dual affinity transporter NRT1.1 (Tomasi et al. 2015). Studies indicate that a LATS linearly contributes to

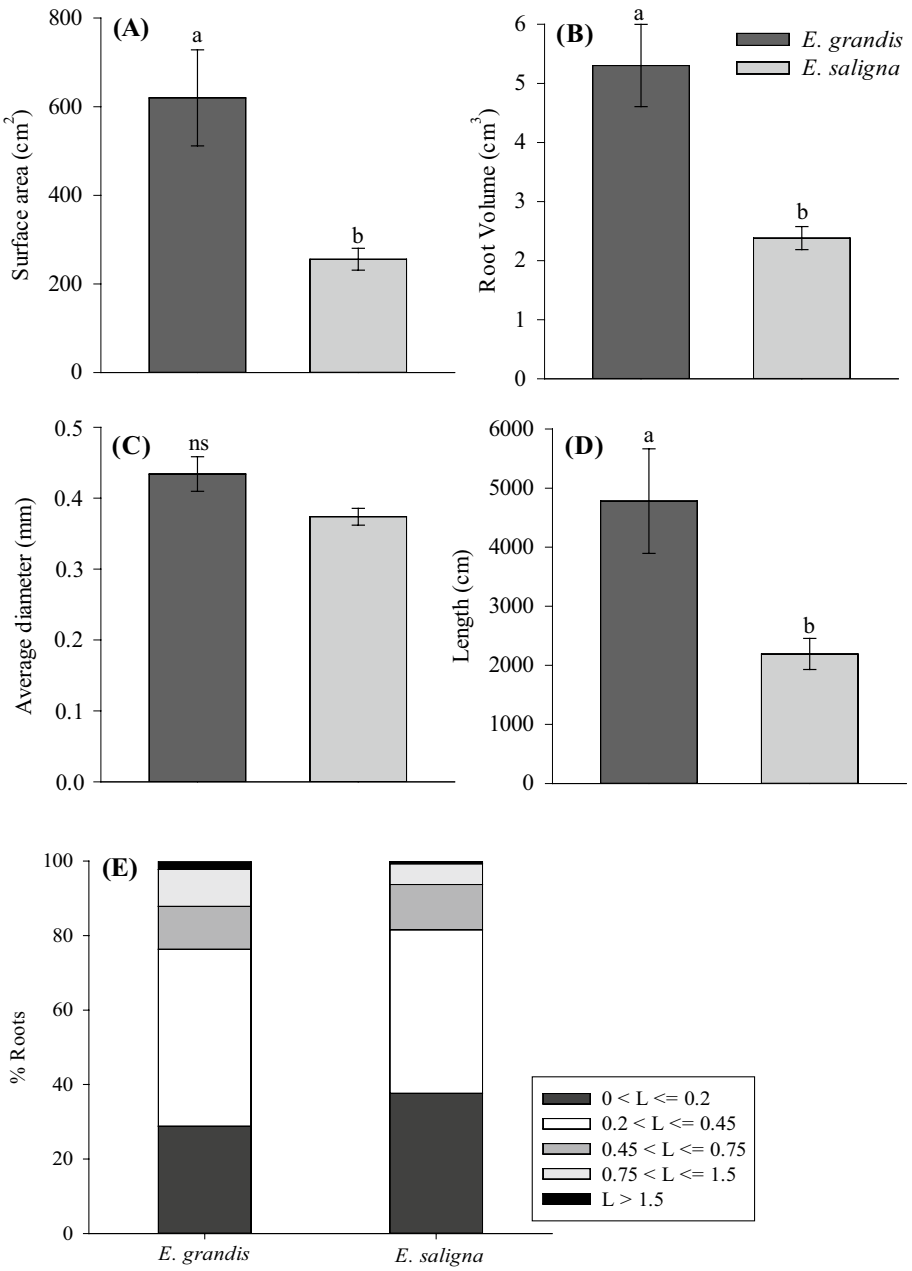

Fig. 1 **a** surface area, **b** root volume, **c** average diameter, **d** length, **e** percent distribution of fine roots for each diameter classes of *E. grandis* and *E. saligna* clones; Means followed by the same letter did not differ by Student's *t*-test ($P < 0.05$)

the absorption of NO_3^- at concentrations above 250 µmol L^{-1} and thereafter, the absorption sites become saturated at concentrations close to 50 mmol L^{-1} in *Arabidopsis* plants (Glass 2003). At low concentrations of NO_3^- in solution, two high-affinity transport systems are activated, one of them constitutive (cHATS), with K_m in a range of 6–20 µmol L^{-1}, while another induced system (iHATS) of lower affinity, occurs with K_m between 20–100 µmol L^{-1} (Tomasi et al. 2015). Responses similar to these were reported by de Paula et al. (2018) who observed that peach rootstocks have different NO_3^- transport systems (HATS and LATS), showing that the same cultivar can act in different NO_3^- transport systems.

The *E. grandis* clone had lower values for K_m and C_{min} of NH_4^+ (Fig. 2b) and higher values for length, surface area and volume of roots compared to the *E. saligna* clone (Fig. 1). These results suggest that the *E. grandis* clone may possibly have a larger number of NH_4^+ absorption sites per root unit (Pii et al. 2014; Tomasi et al. 2015). Therefore, root morphological parameters are crucial when access to nutrients, including NO_3^- and NH_4^+, is a limiting factor, revealing the adaptability of *Eucalyptus* clone root architecture (Gonçalves et al. 2013).

Accordingly, root morphology contributed to the kinetic NH_4^+ absorption parameters illustrated by the *E. grandis*

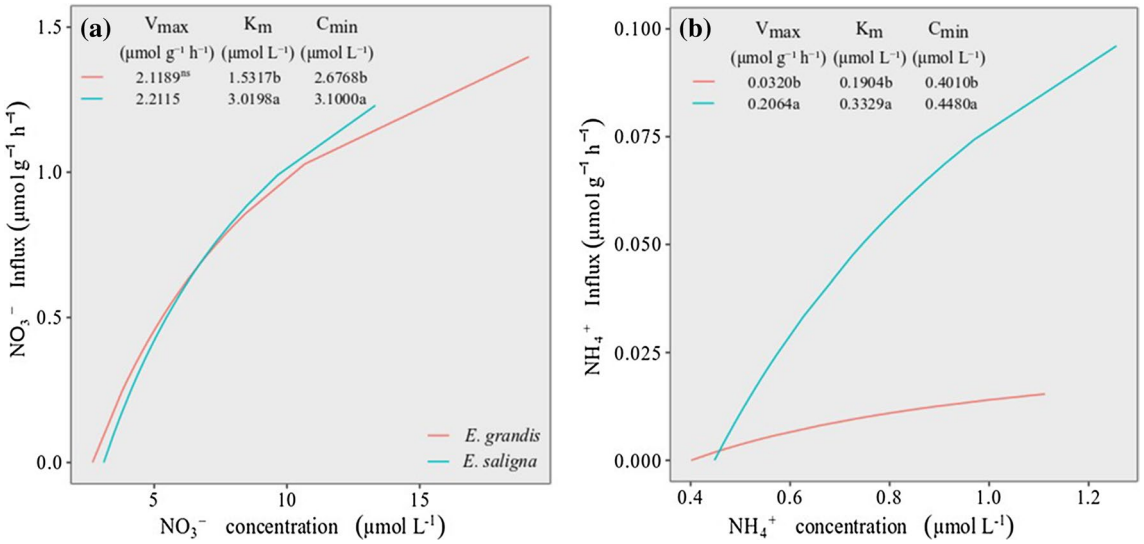

Fig. 2 Influx rates and kinetic parameters of **a** NO_3^- and **b** NH_4^+ uptake of *E. grandis* and *E. saligna* clones; Means followed by the same letter did not differ by Student's *t*-test ($P < 0.05$)

clone and possibly provided higher NH_4^+ uptake due solely to the greater affinity of NH_4^+ transporters, reflected in lower K_m values compared to the *E. saligna* clone (Fig. 2b). The *E. grandis* clone possibly operates in a high affinity transport system, allowing NH_4^+ absorption even when the nutrient is in low concentrations (Couturier et al. 2007; Li et al. 2012). This explains the greater efficiency of the *E. grandis* clone in absorbing NH_4^+ being able to activate NH_4^+ absorption sites, even though the ions are in very low concentrations in solution or the soil, allowing it to reach lower C_{min} values (Fig. 2b). In contrast, higher V_{max} values were observed in the *E. saligna* clone, suggesting that this clone may activate a NH_4^+ low affinity transport system, resulting in higher K_m and C_{min} values. Some studies have reported that ion uptake may be mediated by high and low affinity transporters of the AMT/MEP/Rh (AMT) protein subfamily. The subfamily AMT1 is responsible for the transport of high affinity NH_4^+ and the subfamily AMT2 for the transport of low affinity NH_4^+. AMTs are proteins that activate the transport of NH_4^+ through the plasma membranes, providing the principal path for NH_4^+ influx into the roots (Castro-Rodríguez et al. 2017; Xuan et al. 2017). Another factor that contributed to the absorption of NH_4^+ from the *E. grandis* clone was the higher production of leaf dry matter. This increased the transpiration rate of the plants and the water gradient between the solution and the plants, allowing the nearness of NH_4^+ to the external surface of the roots. This favors its absorption and transport, can accumulate of N in leaves and roots (Table 1) (El-Jendoubi et al. 2013; Jordan et al. 2014; Rivera et al. 2016).

Evaluation of NO_3^- and NH_4^+ absorption over the kinetic gait period

The NO_3^- absorption kinetic gait demonstrated that, initially, the two clones absorbed NO_3^- intensely (Fig. 3), possibly due to low N reserves and high nutrient demand (Tomasi et al. 2015). This NO_3^- decay behavior in solution occurred in a circuitous pattern up to 24-h evaluation, and thereafter the decay occurred smoothly. Similar responses have been reported in NO_3^- absorption studies (Yang et al. 2007; Pii et al. 2014). The sinuous decay of NO_3^- in solution for the clones occurred within 24-h evaluation. This shows that the initial uptake by the *Eucalyptus* clones was similar, and that uptake occurred through a low affinity transport system (LATS). However, the differentiation of root morphological characteristics between clones provided different mechanisms of NO_3^- absorption. After 24 h, the clones possibly initiated the absorption of NO_3^- through another transport system (HATS) until the absorption of NO_3^- decreases, reaching C_{min}, showing the highest absorption efficiency of the *E. grandis* clone. This allowed for the absorption of NO_3^- in low concentrations in solution. As a result, lower values of K_m and C_{min} were achieved. The *E. saligna* clone absorbed NO_3^- less intensely, reaching C_{min} only after 65-h appraisal (Fig. 3). However, the *E. grandis* clone absorbed NO_3^- more continuously than the other clone, reaching C_{min} at 64-h evaluation. The results show that *Eucalyptus* clones differ in NO_3^- absorption intensity, and this correlates with the genetic characteristics of each clone (Tomasi et al. 2015; Kiba and Krapp 2016).

The NH_4^+ absorption kinetic gait showed that initially absorption occurs similarly in both clones. Initial uptake

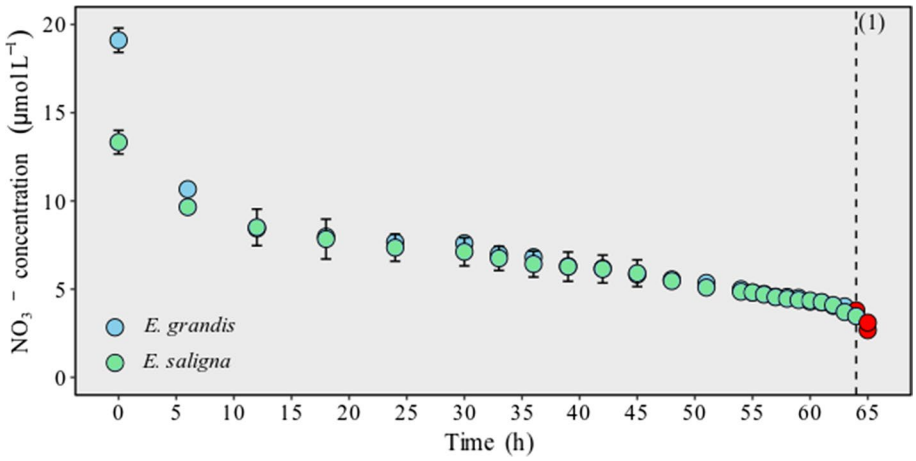

Fig. 3 Concentration of NO_3^- in nutrient solution with *E. grandis* and *E. saligna* clones after 30-d internal nutrient depletion; Average NO_3^- concentrations in blue and green differ significantly from averages of concentrations in red $\alpha = 0.05$ (Scott Knot's test). [a]Time reaching lowest concentration $P < 0.05$

of NH_4^+ is intense by the roots, with a more winding NH_4^+ decay behavior in solution up to 12-h evaluation, and then the decay occurs less intensely until 42-h evaluation (Fig. 4). This possibly was caused by the low induction of proteins that act on the transport of NH_4^+ in the root plasma membranes where the main route of NH_4^+ influx is mediated by NH_4^+ transporter proteins (AMTs). This may occur due to NH_4^+ saturation at these absorption sites, differentiating an initial NH_4^+ depletion stage in the solution between two absorption mechanisms. A low affinity NH_4^+ uptake mechanism possibly occurs up to 12 h in the two clones, which are saturated until near 42-h evaluation. Low affinity NH_4^+ transport is mediated by AMT2 proteins and then another high affinity NH_4^+ uptake mechanism activates, thus activating NH_4^+ transporter proteins (AMT1) (Castro-Rodríguez et al. 2017). As a result, the absorption of NH_4^+ by the transporters decreases until reaching C_{min} at 48-h evaluation (Fig. 4) but with a difference in the NH_4^+ concentration in solution which shows the differentiation between the clones regarding ion extraction capacity. This justifies lower values of K_m for *E. grandis* when compared to *E. saligna*.

It should be noted that the clones continued to absorb NO_3^- and NH_4^+ over the 65-h evaluation period and only after 65 h reached C_{min} for NO_3^- and 48 h for NH_4^+. This shows the importance of the collecting solutions at more spaced out periods in the initial hours of absorption, compared with the more 5 h of evaluation as used for cabbage (Song et al., 2016), 8 h for rice (Araújo et al. 2015), 24 h for corn (Horn et al. 2006), and grapes (Tomasi et al. 2015). In addition, at the end of the evaluation period, sampling should be performed in shorter periods so that it is possible to note with more accuracy the actual moment plants reach C_{min}.

Gas exchange parameters

Significantly higher levels of intercellular CO_2 concentration were observed in *E. grandis* (Fig. 5c). This was because the clone had the highest values of accumulated N in leaves and shoot dry matter production. Therefore, the availability of CO_2 was maximized and the assimilation of C from photosynthesis was assisted. This contributed to greater CO_2

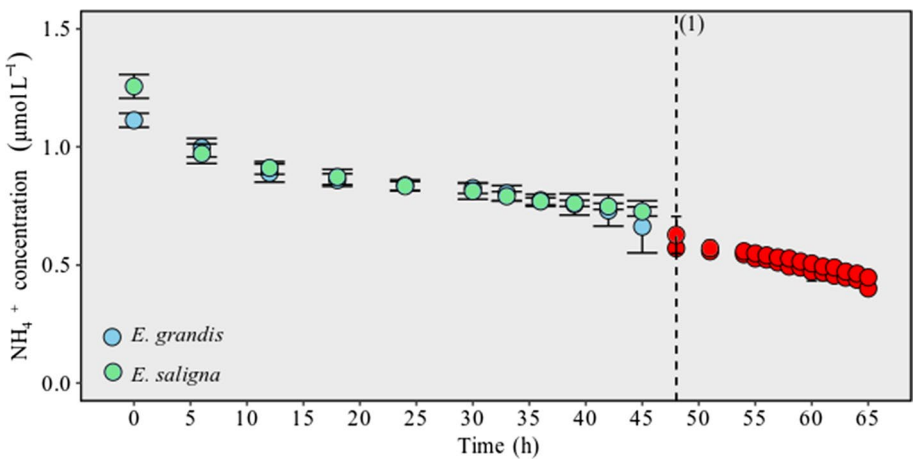

Fig. 4 Concentration of NH_4^+ in nutrient solution with *E. grandis* and *E. saligna* clones after 30-d reduced internal nutrient reserves; Average NH_4^+ concentrations in blue and green differ significantly from averages in red $\alpha = 0.05$ (Scott Knot´s test). [a]Time reaching lowest concentration $P < 0.05$

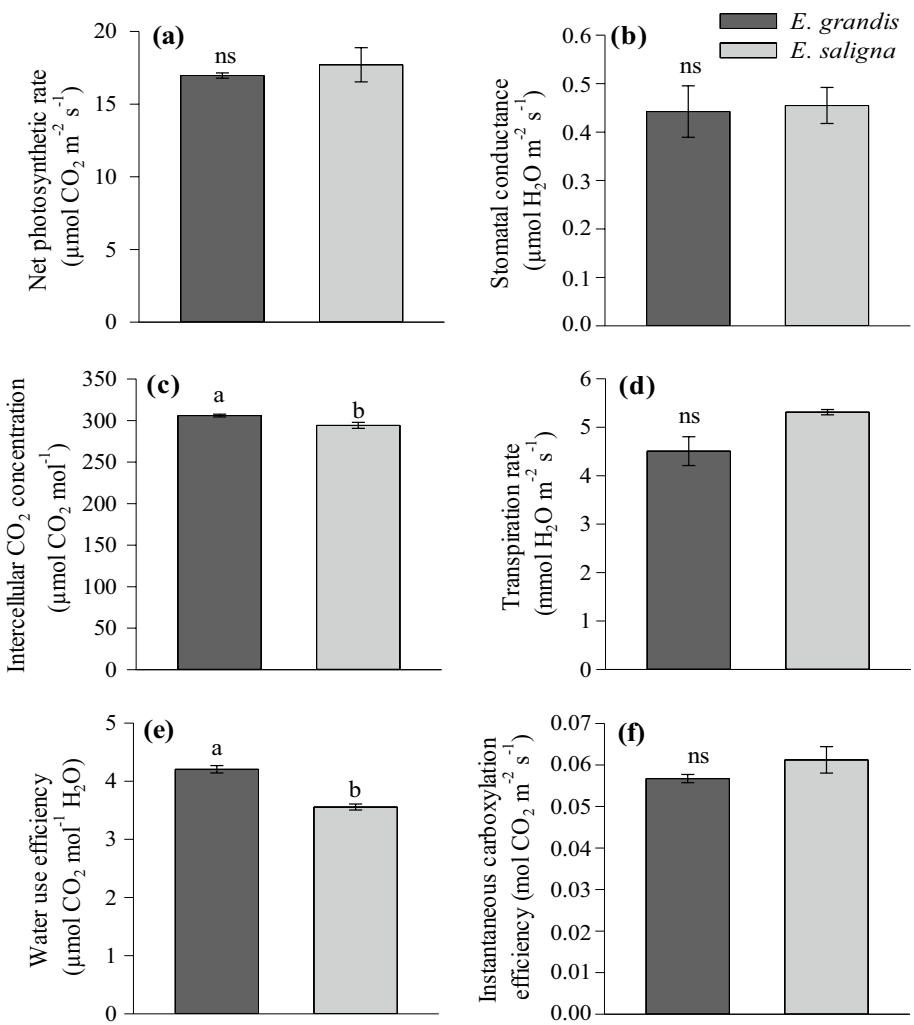

Fig. 5 **a** net photosynthetic rate, **b** stomatal conductance, **c** intercellular CO_2 concentration, **d** transpiration rate, **e** water use efficiency and **f** instantaneous carboxylation efficiency in leaves of *E. grandis* and *E. saligna* clones; Means followed by the same letter did not differ by Student's *t*-test ($P < 0.05$)

fixation in leaf tissues (Martim et al. 2009; Tcherkez et al. 2017). These results corroborate studies with perennial crops which show that the increase in leaf N content correlates with an increase in the CO_2 absorption rate (Jennings et al. 2016; Greer 2018). The results suggest that the *E. grandis* clone converted greater amounts of CO_2 per leaf tissue area, highlighting the importance of clone genotype on photosynthetic parameters (Nadal and Flexas 2018). However, no significant difference was observed between the two clones for net photosynthetic rate (Fig. 5a). However, this higher intercellular CO_2 concentration may be the result of greater respiration (Tcherkez et al. 2017). This confirms the greater efficiency of the *E. grandis* clone in the absorption of NO_3^- and NH_4^+ and, consequently, greater accumulation of N in the leaves and assisting in photosynthesis by contributing important chloroplast proteins (Blank et al. 2018; Hu et al. 2019; Moriwaki et al. 2019).

The *E. grandis* clone showed significantly higher water use efficiency (WUE) than the *E. saligna* clone (Fig. 5e). Although there was no statistical difference in rate of transpiration (Fig. 5d), the *E. grandis* clone lost less H_2O per unit area because transpiration is expressed as mmol H_2O m^{-2} s^{-1}. This may be related to internal CO_2 concentration, resulting in greater leaf vigor which may result in greater WUE (Fig. 5e). In addition, water use efficiency is an important metric for indicating plant stress and demonstrating crop suitability under different edaphoclimatic conditions (Wu et al. 2018). However, the *Eucalyptus* clones did not differ statistically in net photosynthetic rate, stomatal conductance of water vapor, rate of transpiration and instantaneous rubisco carboxylation efficiency (Fig. 5a, b, d, f).

The *E. grandis* clone had the lowest photochemical quenching coefficient (qP) compared to the *E. saligna* clone (Fig. 6a), and consequently had the highest maximum quantum yield of photosystem II (F_v/F_m) and effective quantum efficiency of PSII (Y(II)) (Fig. 6b, d). These results indicate that the *E. grandis* clone transfers more excitation energy from the light collecting system to the reaction center, and more energy directed to the photochemical reaction (Wang et al. 2019). This illustrates

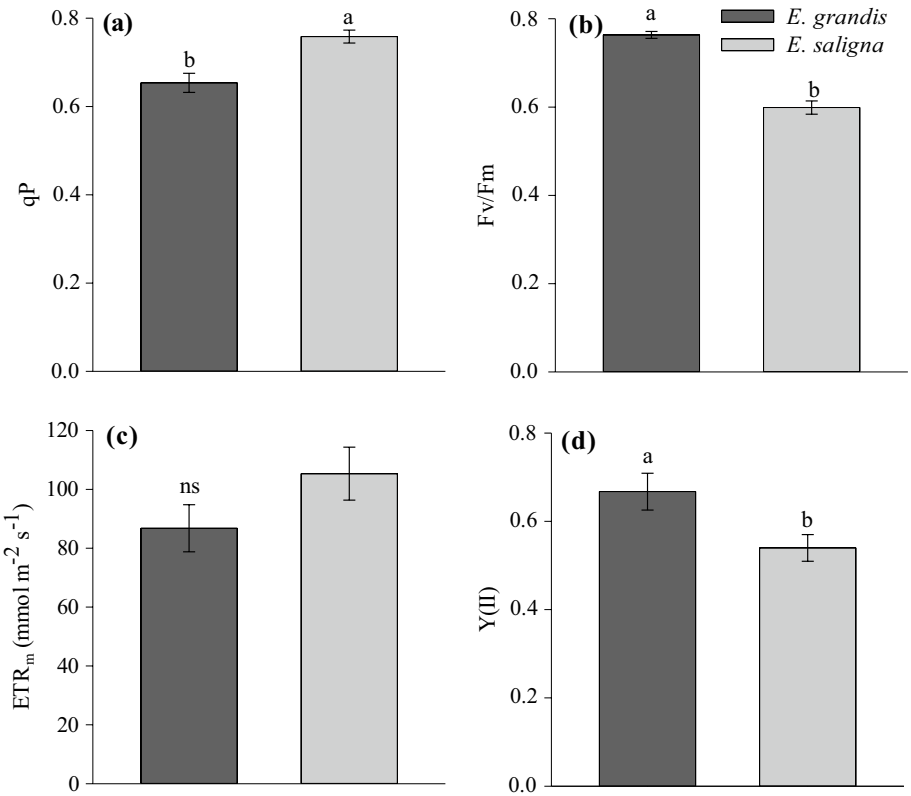

Fig. 6 **a** photochemical quenching coefficient (qP), **b** maximum quantum yield of PSII (F_v/F_m), **c** electron transport rate (ETR_m) and **d** effective quantum efficiency of PSII (Y(II) in *E. grandis* and *E. saligna* clone leaves; Means followed by the same letter did not differ by Student's *t*-test ($P < 0.05$)

that plants with less energy loss reflect higher shoot dry matter production (Table 1). The *E. grandis* clone uses more energy directed to the photochemical stage of photosynthesis, converting more light energy into chemical energy. Therefore, the lower the dissipation of energy in the form of fluorescence, the greater the formation of ATP and NADPH and, consequently, the greater the photosynthetic C assimilation.

The *E. grandis* clone had the highest carotenoid content (Fig. 7), indicating higher levels per leaf area, allowing greater energy absorption and transfer in photosynthesis as carotenoids are responsible for light absorption in different regions of the spectrum in early stages of photosynthesis. In addition, the photochemical phase is only accomplished if there are sufficient pigments to interact with photosynthetic radiation. The higher carotenoid levels in the *E. grandis* may also protect against excess light, as carotenoids, besides acting as accessory pigments, are also photoprotective agents (Marschner 2012). Levels of chlorophyll *a*, *b* and total chlorophyll did not differ statistically between clones (Fig. 7). However, the concentration of photosynthetic pigment contents in the *E. saligna* leaves may be attributed to lower dry matter production (Table 1). Thus, larger amounts of pigments are visualized per unit of mass, resulting in a concentration of photosynthetic pigments, allowing close values between the clones.

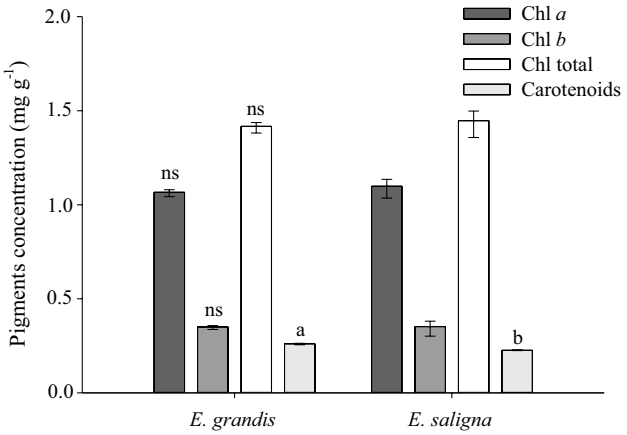

Fig. 7 Pigments concentration of chlorophyll *a* (Chl *a*), chlorophyll *b* (Chl *b*), total chlorophyll (Chl total) and carotenoids in leaves of *E. grandis* and *E. saligna* clones; Means followed by the same letter did not differ by Student's *t*-test ($P < 0.05$)

Principal component analysis (PCA)

PCA was carried out by extracting only the first two components, PC1 and PC2, in which their sum explained 72.95% of the original data variability (Fig. 8). Of this, 53.72% were explained by PC1 and 19.23% by PC2. The PCA results show two clusters of data, highlighting the differentiation of *E. saligna* and *E. grandis* clones. The variables with the

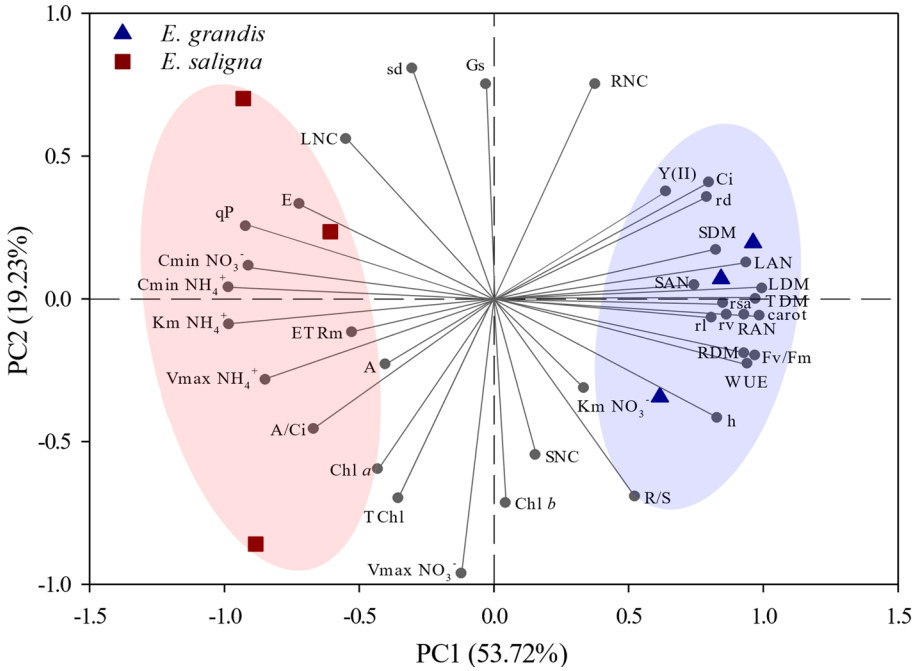

Fig. 8 Scatter plot of principal component analysis (PCA) of kinetic parameters of NO_3^- and NH_4^+ (V_{max}; K_m; C_{min}), morphological (height (h); stem diameter (sd); dry matter in leaves (LDM), in stem (SDM), in roots (RDM), in total (TDM); root/shoot ratio (R/S); total N in leaves (LNC), in stems (SNC), in roots (RNC); N accumulated in leaves (NLA), in stem (NSA), in roots (NRA)), root morphological parameters (surface area (rsa); volume (rv); diameter (rd); length (rl)) and physiological parameters (photochemical quenching coefficient (qP); effective quantum efficiency of PSII (Y(II)); electron transport rate (ETRm); maximum quantum yield of PSII (Fv/Fm); net photosynthetic rate (E); stomatal conductance (Gs); intercellular CO_2 concentration (Ci); transpiration rate (A); water use efficiency (WUE); instantaneous carboxylation efficiency (A/Ci); concentration of chlorophyll *a* (Chl *a*), *b* (Chl *b*), total (Chl total); carotenoids in leaves) in *E. grandis* and *E. saligna* clones

greatest influence on the group formed by the *E. grandis* repetitions were height (h); leaf accumulated N (LAN), stem accumulated nitrogen (SAN) and root accumulated nitrogen (RAN); leaf dry matter (LDM), stem dry matter (SDM), root dry matter (RDM) and total dry matter (TDM); root surface area (RSA), root length (RL), root volume (RV) and root diameter (RD); photosystem II quantum yield (F_v/F_m), maximum fluorescence (F_m), water use efficiency (WUE), CO_2 intercellular concentration (Ci) and carotenoids (carot). In contrast, the *E. saligna* clone was influenced by the variables C_{min} of NO_3^- and NH_4^+, K_m of NH_4^+, V_{max} of NH_4^+, minimum fluorescence (F_o), electron transport rate (ETR_m), net photosynthetic rate (E), stomatal conductance (Gs) and instantaneous carboxylation efficiency (A/Ci).

Kinetic parameters C_{min} of NO_3^- and NH_4^+, K_m of NH_4^+, V_{max} of NH_4^+, were negatively correlated with root morphology, length, diameter, area and volume, and correlated positively with the *E. grandis* clone. This suggests that the higher the development of the *Eucalyptus* clone root system, the lower the C_{min} and V_{max} of NO_3^- and NH_4^+, and K_m of NH_4^+. This is important because the lower their values, the greater the absorption efficiency of NO_3^- and NH_4^+ and the lower the concentration at which roots will be able to extract the nutrient from the solution. In addition, these results demonstrate that as the plant invests photoassimilates in the roots, the likelihood of water and nutrient absorption increases and this results in lower C_{min} values, as plants will be able to access more restricted areas and lower concentrations of elements. Combined with this, in this grouping there is a positive correlation with the increase of nitrogen in the leaves, stem and roots. This confirms the positive correlation carotenoid pigment levels per leaf area which helps the assimilation of intercellular CO_2 provided by quantum yield of photosystem II, thereby assisting the development of the *E. grandis* clone. Thus, higher heights, stem diameters, and leaf, stem and root dry matter production were observed.

Another grouping differentiates the *E. saligna* clone and shows the strong influence of kinetic parameters on the absorption efficiency of different forms of nitrogen and, consequently, the accumulation of N in organs. The *E. saligna* clone was positively correlated with the C_{min} variables of NO_3^- and NH_4^+, K_m of NH_4^+, which is not desirable as it shows a lower affinity for NO_3^- and NH_4^+ absorption. This confirms the positive correlations with physiological parameters such as photosynthetic stress. This suggest that the clone may have suffered damage to the PSII reactive

center, decreasing the efficiency of excitation energy transfer from the light collecting system to the reaction center. This result in lower development of leaves, justifying the inverse correlation with dry matter production (LDM).

Conclusions

The *E. grandis* clone was more efficient in the absorption of NO_3^- and NH_4^+ and had kinetic parameters with lower values of C_{min} and K_m compared to the *E. saligna* clone. Root morphological parameters such as area, volume and length are positively related with kinetic absorption parameters such as lower K_m and C_{min} and can be used in selection and breeding programs of *Eucalyptus*. However, the minimum time for kinetic gait assessment to reach C_{min} for *Eucalyptus* clones should be 65 h for NO_3^- and 48 h for NH_4^+. Kinetic gait studies help in understanding nutrient absorption, and the results of this study may contribute to the selection of more efficient *Eucalyptus* clones in absorbing forms of nitrogen and assist in nitrogen fertilization strategies.

References

Alves LS, Torres CV, Fernandes MS, Santos AMD, Souza SRD (2016) Soluble fractions and kinetics parameters of nitrate and ammonium uptake in sunflower ("Neon" Hybrid). Rev Cienc Agron. https://doi.org/10.5935/1806-6690.20160002

Araújo OJ, Pinto MS, Sperandio MV, Santos LA, Stark EM, Fernandes MS, Santos AM, Souza SR (2015) Expression of the genes OsNRT1.1, OsNRT2.1, OsNRT2.2, and kinetics of nitrate uptake in genetically contrasting rice varieties. Am J Plant Sci. https://doi.org/10.4236/ajps.2015.62035

Batista RO, Furtini Neto AE, Deccetti SFC, Viana CS (2016) Root morphology and nutrient uptake kinetics by Australian cedar clones. Rev Caatinga. https://doi.org/10.1590/1983-21252016v29n118rc

Bednorz D, Tauchnitz N, Christen O, Rupp H, Meissner R (2016) The impact of soil heterogeneity on nitrate dynamic and losses in tile-drained arable fields. Water Air Soil Poll. https://doi.org/10.1007/s11270-016-3095-5

Bindraban PS, Dimkpa C, Nagarajan L, Roy A, Rabbinge R (2015) Revisiting fertilisers and fertilisation strategies for improved nutrient uptake by plants. Biol Fertil Soils. https://doi.org/10.1007/s00374-015-1039-7

Blank M, Tittmann S, Ghozlen NB, Stoll M (2018) Grapevine rootstocks result in differences in leaf composition (*Vitis vinifera* L. cv. Pinot Noir) detected through non-invasive fluorescence sensor technology. Aust J Grape Wine Res. https://doi.org/10.1111/ajgw.12343

Booth TH (2013) Eucalypt plantations and climate change. For Ecol Manag. https://doi.org/10.1016/j.foreco.2012.04.004

Canarini A, Kaiser C, Merchant A, Richter A, Wanek W (2019) Root exudation of primary metabolites: mechanisms and their roles in plant responses to environmental stimuli. Front Plant Sci. https://doi.org/10.3389/fpls.2019.00157

Castro-Rodríguez V, Cañas RA, Torre FN, Pascual MB, Avila C, Cánovas FM (2017) Molecular fundamentals of nitrogen uptake and transport in trees. J Exp Bot. https://doi.org/10.1093/jxb/erx037

Centinari M, Vanden Heuvel JE, Goebel M, Smith MS, Bauerle TL (2016) Root zone management practices impact above and belowground growth in Cabernet Franc grapevines. Aust J Grape Wine R. https://doi.org/10.1111/ajgw.12162

Claassen N, Barber SA (1974) A method for characterizing the relation between nutrient concentration and flux into roots of intact plants. Plant Physiol. https://doi.org/10.1104/pp.54.4.564

Clough T, Condron L, Kammann C, Müller C (2013) A review of biochar and soil nitrogen dynamics. Agronomy. https://doi.org/10.3390/agronomy3020275

Couturier J, Montanini B, Martin F, Brun A, Blaudez D, Chalot M (2007) The expanded family of ammonium transporters in the perennial poplar plant. New Phytol. https://doi.org/10.1111/j.1469-8137.2007.01992.x

de Paula BV, Marques ACR, Rodrigues LAT, de Souza ROS, Kulmann MSD, Kaminski J, Ceretta CA, de Melo GWB, Mayer NA, Antunes LE, Ricachenevsky FK, Nicoloso FT, Brunetto G (2018) Morphological and kinetic parameters of the uptake of nitrogen forms in clonal peach rootstocks. Sci Hortic. https://doi.org/10.1016/j.scienta.2018.05.038

Doddema H, Telkamp GP (1979) Uptake of nitrate by mutants of *Arabidopsis thaliana*, disturbed in uptake or reduction of nitrate: II. Kinetics Physiol Plant. https://doi.org/10.1111/j.1399-3054.1979.tb02593.x

Dechorgnat J, Nguyen CT, Armengaud P, Jossier M, Diatloff E, Filleur S, Vedele DF (2010) From the soil to the seeds: the long journey of nitrate in plants. J Exp Bot. https://doi.org/10.1093/jxb/erq409

El-Jendoubi H, Abadía J, Abadía A (2013) Assessment of nutrient removal in bearing peach trees (*Prunus persica* L. Batsch) based on whole tree analysis. Plant Soil. https://doi.org/10.1007/s11104-012-1556-1

FAO (2016) Food and agriculture organization of the United Nations. Global Forest Resources Assessment 2015: How are the World's Forests Changing? 2ed. Roma: FAO, 2016. p. 54.

Glass ADM (2003) Nitrogen use efficiency of crop plants: physiological constraints upon nitrogen absorption. CR Rev Plant Sci. https://doi.org/10.1080/07352680390243512

Gonçalves JLM, Alvares CA, Higa AR, Silva LD, Alfenas AC, Stahl J, Bouillet JPD (2013) Integrating genetic and silvicultural strategies to minimize abiotic and biotic constraints in Brazilian eucalypt plantations. For Ecol Manag. https://doi.org/10.1016/j.foreco.2012.12.030

Greer DH (2018) Photosynthetic responses to CO_2 at different leaf temperatures in leaves of apple trees (*Malus domestica*) grown in orchard conditions with different levels of soil nitrogen. Environ Exp Bot. https://doi.org/10.1016/j.envexpbot.2018.06.014

Hiscox JD, Israelstam GF (1979) A method for the extraction of chlorophyll from leaf tissue without maceration. Can J Bot. https://doi.org/10.1139/b79-163

Horn D, Ernani P, Sangoi L, Schweitzer C, Cassol PC (2006) Parâmetros cinéticos e morfológicos da absorção de nutrientes em cultivares de milho com variabilidade genética contrastante. Rev Bras Cienc Solo 30: 77–85. https://www.redalyc.org/pdf/1802/180214052009.pdf

Hu YT, Zhao P, Zhu LW, Zhao XH, Ni GY, Ouyang L, Schafer KVR, Shen WJ (2019) Responses of sap flux and intrinsic water use efficiency to canopy and understory nitrogen addition in a temperate broadleaved deciduous forest. Sci Total Environ. https://doi.org/10.1016/j.scitotenv.2018.08.158

Iglesias G, Wilstermann D (2008) *Eucalyptus* universalis. Global cultivated eucalypt forests map. <https://git-forestry-blog.blogspot.com/2008/09/eucalyptus-global-map-2008-cultivated.html> [accessed 21.12.18].

Jennings KA, Guerrieri R, Vadeboncouer MA, Asbjornsen H (2016) Response of *Quercus velutina* growth and water use efficiency to climate variability and nitrogen fertilization in a temperate

deciduous forest in the northeastern USA. Tree Physiol. https://doi.org/10.1093/treephys/tpw003
Jones B (1983) A guide for the hydroponic and soilless culture grower. Timber Press 194–195.
Jordan MO, Vercambre G, Gomez L, Pages L (2014) The early spring N uptake of young peach trees (*Prunus persica*) is affected by past and current fertilizations and levels of C and N stores. Tree Physiol. https://doi.org/10.1093/treephys/tpt109
Kiba T, Krapp A (2016) Plant nitrogen acquisition under low availability: Regulation of uptake and root architecture. Plant Cell Physiol. https://doi.org/10.1093/pcp/pcw052
Klodd AE, Eissenstat DM, Wolf TK, Centinari M (2016) Coping with cover crop competition in mature grapevines. Plant Soil. https://doi.org/10.1007/s11104-015-2748-2
Kronzucker HJ, Siddiqi MY, Glass AD (1995) Kinetics of NO_3^- influx in spruce. Plant Physiol. https://doi.org/10.1104/pp.109.1.319
Lambers H, Shane MW, Cramer MD, Pearse SJ, Veneklaas EJ (2006) Root structure and functioning for efficient acquisition of phosphorus: matching morphological and physiological traits. Ann Bot-London. https://doi.org/10.1093/aob/mcl114
Lee HJ, Ha JH, Kim SG, Choi HK, Kim ZH, Han YJ, Hyeon T (2016) Stem-piped light activates phytochrome B to trigger light responses in *Arabidopsis thaliana* roots. Sci Signal. https://doi.org/10.1126/scisignal.aaf6530
Li H, Li MC, Luo J, Cao X, Qu L, Gai Y, Jiang XN, Liu TX, Bai H, Janz D, Polle A, Peng CH, Luo ZB (2012) N-fertilization has different effects on the growth, carbon and nitrogen physiology, and wood properties of slow- and fast-growing *Populus* species. J Exp Bot. https://doi.org/10.1093/jxb/ers271
Lichtenthaler HK (1987) Chlorophylls and carotenoids: pigments of photosynthetic biomembranes. Method Enzymol 148:350–382
Martim SA, Santos MP, Peçanha AL, Pommer C, Campostrini E, Viana AP, Bressan-Smith R (2009) Photosynthesis and cell respiration modulated by water deficit in grapevine (*Vitis vinifera* L.) cv. Cabernet Sauvignon Braz J Plant Physiol. https://doi.org/10.1590/S1677-04202009000200002
Martinez HE, Olivos A, Brown PH, Clemente JM, Bruckner CH, Jifon JL (2015) Short-term water stress affecting NO_3^- absorption by almond plants. Sci Hortic. https://doi.org/10.1016/j.scienta.2015.10.040
Marschner P (2012) Marschner's Mineral Nutrition of Higher Plants, 5th edn. Elsevier, Academic Press, Cambridge, p 651
Moriwaki T, Falcioni R, Tanaka FAO, Cardoso KAK, Souza LA, Benedito E, Nanni NR, Bonato CM, Antunes WC (2019) Nitrogen-improved photosynthesis quantum yield is driven by increased thylakoid density, enhancing green light absorption. Plant Sci. https://doi.org/10.1016/j.plantsci.2018.10.012
Nadal M, Flexas J (2018) Variation in photosynthetic characteristics with growth form in a water-limited scenario: Implications for assimilation rates and water use efficiency in crops. Agr Water Manage. https://doi.org/10.1016/j.agwat.2018.09.024
Nielsen NE, Barber SA (1978) Differences among genotypes of corn in the kinetics of P uptake[1]. Agronomy J. https://doi.org/10.2134/agronj1978.00021962007000050001xa
Ortega RA, Westfall DG, Gangloff WJ, Peterson GA, Stafford J (1999) Multivariate approach to N and P recommendations in variable rate fertilizer applications. Precis Agric 99:387–396
Paquette A, Messier C (2010) The role of plantations in managing the world's forests in the Anthropocene. Front Ecol Environ 8:27–34
Pii Y, Alessandrini M, Guardini K, Zamboni A, Varanini Z (2014) Induction of high-affinity NO_3^- uptake in grapevine roots is an active process correlated to the expression of specific members of the NRT2 and plasma membrane H+-ATPase gene families. Funct Plant Biol. https://doi.org/10.1071/FP13227
R Development Core Team (2019) R: a language and environment for statistical computing. https://www.R-Project.Org/.
Raven JA, Lambers H, Smith SE, Westoby M (2018) Costs of acquiring phosphorus by vascular land plants: patterns and implications for plant coexistence. New Phytol. https://doi.org/10.1111/nph.14967
Rivera R, Bañados P, Ayala M (2016) Distribution of 15N applied to the soil in the "Bing"/"Gisela®6" sweet cherry (*Prunus avium* L.) combination. Sci Hortic. https://doi.org/10.1016/j.scienta.2016.06.035
Rocha JDG, Ferreira LM, Tavares OCH, Santos AMD, Souza SRD (2014) Cinética de absorção de nitrogênio e acúmulo de frações solúveis nitrogenadas e açúcares em girasol. Pesqui Agropecu Trop. https://doi.org/10.1590/S1983-40632014000400009
Schreiber UBWN, Bilger W, Neubauer C (1995) Chlorophyll fluorescence as a nonintrusive indicator for rapid assessment of in vivo photosynthesis. In: Schulze E, Caldwell MM (Eds) Ecophysiology of photosynthesis. Springer, Berlin, pp 49–70. https://doi.org/10.1007/978-3-642-79354-7_3
Skaggs TH, Shouse PJ (2008) Roots and root function: introduction. Vad Z J. https://doi.org/10.2136/vzj2008.0076
Song SW, Li G, Sun GW, Liu HC, Chen RY (2016) Uptake kinetics of different nitrogen forms by Chinese kale. Commun Soil Sci Plan. https://doi.org/10.1080/00103624.2016.1178279
Souza TC, Magalhães PC, Castro EM, Albuquerque PEP, Marabesi MA (2013) The influence of ABA on water relation, photosynthesis parameters, and chlorophyll fluorescence under drought conditions in two maize hybrids with contrasting drought resistance. Acta Physiol Plant. https://doi.org/10.1007/s11738-012-1093-9
Tcherkez G, Gauthier P, Buckley TN, Busch FA, Barbour MM, Bruhn D, Way D (2017) Leaf day respiration: low CO_2 flux but high significance for metabolism and carbon balance. New Phytol. https://doi.org/10.1111/nph.14816
Ter Braak CJ, Smilauer P (2002) CANOCO reference manual and CanoDraw for Windows user's guide: software for canonical community ordination (version 4.5). www.canoco.com.
Tomasi N, Monte R, Varanini Z, Cesco S, Pinton R (2015) Induction of nitrate uptake in Sauvignon Blanc and Chardonnay grapevines depends on the scion and is affected by the rootstock. Aust J Grape Wine Res. https://doi.org/10.1111/ajgw.12137
Wang H, Zhang HH, Liu YS, Long JH, Meng L, Xu N, Li JB, Zhong HX, Wu YN (2019) Increase of nitrogen to promote growth of poplar seedlings and enhance photosynthesis under NaCl stress. J For Res. https://doi.org/10.1007/s11676-018-0775-6
Wu ZZ, Ying YQ, Zhang YB, Bi YF, Wang AK, Du XH (2018) Alleviation of drought stress in *Phyllostachys edulis* by N and P application. Sci Rep 8:228
Xuan W, Beeckman T, Xu GH (2017) Plant nitrogen nutrition: sensing and signaling. Curr Opin Plant Biol. https://doi.org/10.1016/j.pbi.2017.05.010
Yang TY, Zhu LN, Wang SP, Gu WJ, Huang DF, Xu WP, Jiang AL, Li SC (2007) Nitrate uptake kinetics of grapevine under root restriction. Sci Hortic. https://doi.org/10.1016/j.scienta.2006.11.005
Zufferey V, Murisier F, Belcher S, Lorenzini F, Vivin P, Spring JL, Viret O (2015) Nitrogen and carbohydrate reserves in the grapevine (*Vitis vinifera* L. 'Chasselas'): the influence of the leaf to fruit ratio. Vitis. https://doi.org/10.5073/vitis.2015.54.183-188